EAI Endorsed Transactions
on Scalable Information Systems
Research Article EAI.EU

Research of IoT Technology Based Online Status Monitoring on Hydropower Station Equipment

Yuanjiang Ma[1], Xudong Lu[1], Liang Hong[1], Xuan He[1], Mianqian Qiu[1], Mingliang Tang[1], and Lei Chen[1,*]

[1]Yingxiuwan Hydropower General Plant of State Grid Sichuan Electric Power Company, Chengdu, 611800, Sichuan, China

Abstract

The rapid proliferation of Internet of Things (IoT) has revolutionized the field of status monitoring for electrical equipment such as hydropower station equipment, offering enhanced efficiency and reliability in maintenance and operations. In this paper, we investigate the utilization of IoT transmission technology enhanced by multiple relays, denoted as M relays, to augment the monitoring of hydropower station equipment. To optimize the performance of the system, we employ partial relay selection, commonly referred to as selection combining. This study delves into the analysis of the system performance by deriving an analytical data rate, with a focus on quantifying the benefits of employing partial relay selection in IoT transmission for electrical equipment status monitoring. Our analytical approach enables a comprehensive evaluation of system efficiency, considering factors such as data rate, reliability, and power consumption. Through our analysis, we aim to provide valuable insights into the trade-offs and advantages of incorporating partial relay selection into IoT systems. By examining the impact of M relays and partial relay selection on IoT transmission technology, the work in this paper can help enhance the reliability of status monitoring for electrical equipment, ultimately advancing the capabilities of IoT-based solutions in the context of electrical systems and equipment maintenance.

Received on 08 December 2023; accepted on 03 March 2023; published on 05 March 2024

Keywords: IoT, online status monitoring, relay selection, analytical data rate.

doi:10.4108/eetsis.4559

1. Introduction

Internet of Things (IoT) networks have ushered in a new era of connectivity and automation, offering transformative capabilities across a wide spectrum of applications [1–4]. Among these, status monitoring within industrial IoT (IIoT) networks stands out as a pivotal domain. Industrial IoT networks provide the infrastructure for real-time, data-driven insights and control over machinery, equipment, and processes within various industrial sectors [5–8]. This includes predictive maintenance in manufacturing plants, remote monitoring of critical infrastructure, and efficient asset management in smart cities. These applications not only enhance operational efficiency but also contribute to cost reduction, improved safety, and sustainability. Through the seamless integration of sensors, data analytics, and network connectivity, IIoT networks empower industries to proactively monitor and manage their assets, minimizing downtime and maximizing productivity [9–12]. As industries continue to embrace the potential of IoT, the development of robust and reliable status monitoring solutions remains at the forefront of innovation, driving advancements in industrial automation and optimization.

Relaying techniques have emerged as a crucial strategy for enhancing the performance of IoT networks, with a profound impact on critical metrics such as data rate, outage probability, and symbol error rate [13–16]. By employing multiple relay nodes strategically within the network architecture, data can be transmitted more reliably and efficiently over extended

*Corresponding author. Email: cchen11@126.com.

distances. These relays act as intermediaries, amplifying and forwarding data, mitigating signal degradation, and reducing the probability of data loss or communication interruptions. Consequently, data rates are substantially improved, enabling IoT networks to support bandwidth-intensive applications and services [17–21]. Moreover, the use of relaying techniques can help reduce the outage probability, ensuring that data transmission remains robust even in challenging environments. Symbol error rates are also investigated as relay nodes enable signal regeneration and error correction, resulting in higher data integrity. This synergy between relaying techniques and IoT networks plays a pivotal role in realizing the full potential of IoT applications, particularly in scenarios where reliability, data rates, and error rates are of paramount importance, such as in critical infrastructure monitoring and healthcare systems [22–26].

Partial relay selection is a key optimization technique within relaying networks, offering significant improvements in data rate, outage probability, and symbol error rate. By carefully selecting a subset of relay nodes from the available pool, this approach intelligently leverages the best-performing relays to amplify and forward data, thereby boosting the data rate. This selective relay strategy not only conserves network resources but also minimizes the interference, resulting in a higher throughput for data transmission. Moreover, partial relay selection reduces the outage probability by dynamically choosing relays that maximize signal quality, ensuring reliable communication, even in challenging conditions. Symbol error rates are also markedly improved through the judicious selection of relays, as only the most favorable relay nodes are employed, reducing the likelihood of symbol errors and enhancing overall data integrity. In essence, partial relay selection is a powerful tool for optimizing the performance of relaying networks, offering an elegant balance between the data rate enhancement, outage probability reduction, and symbol error rate minimization, thereby rendering it indispensable for various communication applications, from wireless sensor networks to next-generation wireless systems.

This paper explores the integration of IoT transmission technology enriched by a set of M relays to enhance the monitoring of electrical equipment. To optimize the system performance, we implement the partial relay selection, often referred to as selection combining. Our investigation delves deep into system performance analysis, primarily focusing on the quantification of the advantages stemming from the integration of partial relay selection in IoT transmission for monitoring the status of electrical equipment. Our analytical approach facilitates a comprehensive assessment of system efficiency, taking into account the transmission data rate. Through our analysis, we endeavor to offer valuable insights into the trade-offs and benefits associated with the incorporation of partial relay selection into IoT systems, ultimately aiding in the development of more efficient solutions for electrical equipment status monitoring. By assessing the impact of M relays and partial relay selection on IoT transmission technology, this research contributes to ongoing efforts aimed at enhancing the reliability and resilience of status monitoring for electrical equipment, thereby advancing the capabilities of IoT-based solutions in the realm of electrical systems and equipment maintenance.

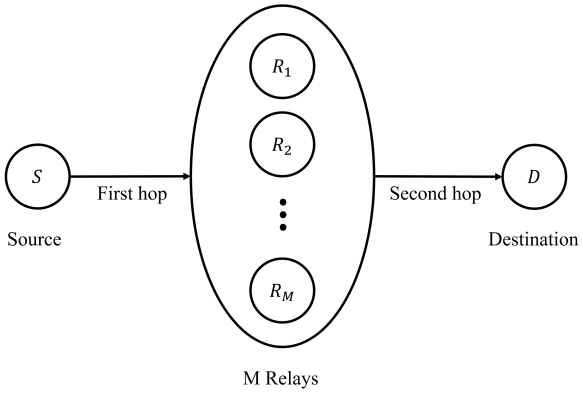

Figure 1. System model of channel-noise-assisted cooperative IoT networks with one transmit source S, M relays, and one destination D.

2. System model

Fig. 1 provides a comprehensive illustration of the system model for channel-noise-assisted cooperative IoT networks. Within this framework, we have a configuration consisting of a single transmitting source, denoted as S, a set of M relays, and a designated destination labeled as D. This network operates on a dual-hop basis, where the source node S initially dispatches a signal to one of the M relays. Subsequently, the selected relay, denoted as m and belonging to the set $\mathcal{M}$, takes charge of transmitting the signal to the destination D. It is essential to note that, for this specific network, we have employed the amplify-and-forward (AF) relaying protocol. Moreover, the relay selection process hinges on identifying the relay within the set $\mathcal{M}$ that exhibits the highest signal-to-noise ratio (SNR) during the second hop of the transmission process. Then, the end-to-end SNR of the cooperative networks with relay selection (RS) is expressed as

$$\omega^{RS} = \frac{\omega_{SR_\eta}\omega_{R_\eta D}}{1 + \omega_{SR_\eta} + \omega_{R_\eta D}}, \tag{1}$$

where R_η denotes the selected relay of total M relays based on $\omega_\eta = \max_{n\in M}\{\omega_{R_n D}\}$, and $\omega_{R_n D}$ represents the instantaneous SNR of the wireless channel from relay R_n to the destination D. Notation ω_{SR_η} denotes the

instantaneous SNR from source S to relay R_η. Then, the probability density functions (PDFs) of ω_{SR_η} and $\omega_{R_\eta D}$ are respectively expressed as

$$f_{\omega_{SR_\eta}}(\omega) = \frac{1}{\alpha_1} e^{-\frac{\omega}{\alpha_1}} \mathrm{V}(\omega), \tag{2}$$

$$f_{\omega_{R_\eta D}}(\omega) = \frac{M}{\alpha_2} \sum_{n=0}^{M-1} \binom{M-1}{n} (-1)^n e^{-\frac{(n+1)\omega}{\alpha_2}} \mathrm{V}(\omega), \tag{3}$$

where $\mathrm{V}(\cdot)$ is the unit step function, and α_1 and α_2 are the average SNR of ω_{SR_η} and $\omega_{R_\eta D}$, respectively.

3. Capacity Analysis

Capacity analysis in the context of channel-noise-assisted cooperative IoT networks is a fundamental aspect of evaluating the network performance and efficiency. This analysis involves the determination of the maximum achievable data rate, or capacity, under specific network conditions. By taking into account the factors such as the number of relays, channel impairments, signal-to-noise ratios, and modulation schemes, we can assess the network ability to transmit data reliably and efficiently. Capacity analysis aids in understanding the limits of information transfer within the network and provides valuable insights for optimizing the system. It is a critical tool for designing and fine-tuning relaying IoT networks, ensuring that they meet the data rate requirements while maintaining a balance between the spectral efficiency and reliability, ultimately enabling robust and high-performing communication in IoT applications. The ergodic capacity of the relaying network with the relay selection is written as

$$C = \frac{1}{2} E_{\omega^{RS}} \{\log_2(1 + \omega^{RS})\}. \tag{4}$$

Based on eq. (1), we write eq. (4) as

$$C = \frac{1}{2} E_{\omega^{SC}} \left\{ \log_2 \frac{(1 + \omega_{R_\eta D})(1 + \omega_{SR_\eta})}{1 + \omega_{SR_\eta} + \omega_{R_\eta D}} \right\} \tag{5}$$

$$= \frac{1}{2\ln 2} E_{\omega_{SR_\eta}} \left\{ \ln(1 + \omega_{SR_\eta}) \right\} + \frac{1}{2\ln 2} E_{\omega_{R_\eta D}} \left\{ \ln(1 + \omega_{R_\eta D}) \right\} - \frac{1}{2\ln 2} E_{\omega_{SR_\eta} + \omega_{R_\eta D}} \left\{ \ln(1 + \omega_{SR_\eta} + \omega_{R_\eta D}) \right\}. \tag{6}$$

Then, we use the PDF of ω_{SR_η} in eq. (2), and derive $E_{\omega_{SR_\eta}} \left\{ \ln(1 + \omega_{SR_\eta}) \right\}$ as

$$E_{\omega_{SR_\eta}} \{\ln(1 + \omega_{SR_\eta})\} = \int_0^\infty \frac{1}{\alpha_1} e^{-\frac{\omega}{\alpha_1}} \ln(1 + \omega) dr \tag{7}$$

$$= \int_0^\infty -\ln(1 + \omega) de^{-\frac{\omega}{\alpha_1}} \tag{8}$$

$$= e^{\frac{1}{\alpha_1}} \int_{\frac{1}{\alpha_1}}^\infty e^{-u} \frac{1}{u} du \tag{9}$$

$$= e^{\frac{1}{\alpha_1}} E_1(\frac{1}{\alpha_1}), \tag{10}$$

where $E_1(x) = \int_x^\infty \frac{1}{x} e^{-x} dx$ is the exponential integral function.

We further utilize the PDF of ω_{SR_η} in eq. (3), and derive $E_{\omega_{R_\eta D}} \left\{ \ln(1 + \omega_{R_\eta D}) \right\}$ as

$$E_{\omega_{R_\eta D}} \left\{ \ln(1 + \omega_{R_\eta D}) \right\} \tag{11}$$

$$= \frac{M}{\alpha_2} \sum_{n=0}^{M-1} \binom{M-1}{n} (-1)^n \int_0^\infty e^{-\frac{(n+1)\omega}{\alpha_2}} \ln(1 + \omega) d\omega \tag{12}$$

$$= M \sum_{n=0}^{M-1} \binom{M-1}{n} \frac{(-1)^n}{n+1} e^{\frac{n+1}{\alpha_2}} \int_{\frac{n+1}{\alpha_2}}^\infty e^{-u} \frac{1}{u} du \tag{13}$$

$$= M \sum_{n=0}^{M-1} \binom{M-1}{n} \frac{(-1)^n}{n+1} e^{\frac{n+1}{\alpha_2}} E_1(\frac{n+1}{\alpha_2}). \tag{14}$$

Now, we turn to derive $E_{\omega_{SR_\eta} + \omega_{R_\eta D}} \left\{ \ln(1 + \omega_{SR_\eta} + \omega_{R_\eta D}) \right\}$ of eq. (4). For this, we first derive the pdf of $\omega_{SR_\eta} + \omega_{R_\eta D}$. Let $\otimes$ denote the convolutional operation, and then the PDF of $\omega_{SR_\eta} + \omega_{R_\eta D}$ can be derived as

$$f_{\omega_{SR_\eta} + \omega_{R_\eta D}}(\omega) = f_{\omega_{SR_\eta}}(\omega) \otimes f_{\omega_{R_\eta D}}(\omega) \tag{15}$$

$$= \int_0^\omega f_{\omega_M}(x) f_{\omega_{SR_\eta}}(r - x) dx \tag{16}$$

$$= \int_0^\omega \frac{M}{\alpha_2} \sum_{n=0}^{M-1} \binom{M-1}{n} (-1)^n e^{-\frac{(n+1)x}{\alpha_2}} \frac{1}{\alpha_1} e^{-\frac{\omega - x}{\alpha_1}} dx \tag{17}$$

$$= \frac{M}{\alpha_1 \alpha_2} \sum_{n=0}^{M-1} \binom{M-1}{n} (-1)^n e^{-\frac{\omega}{\alpha_1}} \int_0^\omega e^{-(\frac{n+1}{\alpha_2} - \frac{1}{\alpha_1})x} dx. \tag{18}$$

Let $m = \frac{\alpha_1}{\alpha_2} - 1$, and u_{nm} denotes

$$f_{\omega_{SR_M} + \omega_{R_\eta D}}(\omega) \tag{22}$$

$$= \frac{M}{\alpha_1 \alpha_2} \sum_{n=0}^{M-1} \binom{M-1}{n} (-1)^n e^{-\frac{\omega}{\alpha_1}} \int_0^\omega dx \tag{23}$$

$$= \frac{M}{\alpha_1 \alpha_2} \sum_{n=0}^{M-1} \binom{M-1}{n} (-1)^n e^{-\frac{\omega}{\alpha_1}} \omega \tag{24}$$

$$
\begin{aligned}
f_{\omega_{SR_\eta}+\omega_{R_\eta D}}(\omega) &= \frac{M}{\alpha_1\alpha_2}\Bigg\{\sum_{n=0}^{M-1} u_{nm}(n-m)\binom{M-1}{n}(-1)^n e^{-\frac{\omega}{\alpha_1}}\int_0^{\omega} e^{-(\frac{n+1}{\alpha_2}-\frac{1}{\alpha_1})x}dx + \Big[1-u_{nm}(n-m)\Big]\binom{M-1}{n}(-1)^n e^{-\frac{\omega}{\alpha_1}}\omega\Bigg\} \\
&= \frac{M}{\alpha_1\alpha_2}\Bigg\{\sum_{n=0}^{M-1} u_{nm}(n-m)\binom{M-1}{n}(-1)^n e^{-\frac{\omega}{\alpha_1}}\frac{e^{-(\frac{n+1}{\alpha_2}-\frac{1}{\alpha_1})x}}{\frac{n+1}{\alpha_2}-\frac{1}{\alpha_1}}\Big|_{\omega}^{0} + \Big[1-u_{nm}(n-m)\Big]\binom{M-1}{n}(-1)^n e^{-\frac{\omega}{\alpha_1}}\omega\Bigg\} \\
&= \frac{M}{\alpha_1\alpha_2}\Bigg\{\sum_{n=0}^{M-1} u_{nm}(n-m)\binom{M-1}{n}(-1)^n e^{-\frac{\omega}{\alpha_1}}\frac{1-e^{-(\frac{n+1}{\alpha_2}-\frac{1}{\alpha_1})\omega}}{\frac{\alpha_1(n+1)-\alpha_2}{\alpha_1\alpha_2}} + \Big[1-u_{nm}(n-m)\Big]\binom{M-1}{n}(-1)^n e^{-\frac{\omega}{\alpha_1}}\omega\Bigg\} \\
&= \sum_{n=0}^{M-1}\frac{u_{nm}}{\alpha_1}\binom{M-1}{n}(-1)^n M\Big[e^{-\frac{\omega}{\alpha_1}} - e^{-\frac{n+1}{\alpha_2}\omega}\Big] + \Big[1-u_{nm}(n-m)\Big]\binom{M-1}{n}\frac{(-1)^n M}{\alpha_1\alpha_2}e^{-\frac{\omega}{\alpha_1}}\omega.
\end{aligned}
\tag{19}
$$

$$
\begin{aligned}
&E_{\omega_{SR_M}+\omega_{R_\eta D}}\left\{\ln\left(1+\omega_{SR_M}+\omega_{R_\eta D}\right)\right\} \\
&= \sum_{n=0}^{M-1}\frac{u_{nm}}{\alpha_1}\binom{M-1}{n}(-1)^n M\left[\alpha_1 e^{\frac{1}{\alpha_1}}E_1(\frac{1}{\alpha_1}) - \frac{\alpha_2}{n+1}e^{\frac{n+1}{\alpha_2}}E_1(\frac{n+1}{\alpha_2})\right] + [1-u_{nm}(n-m)]\binom{M-1}{n}\frac{(-1)^n M}{\alpha_2}\left[\alpha_1+(\alpha_1-1)e^{\frac{1}{\alpha_1}}E_1(\frac{1}{\alpha_1})\right].
\end{aligned}
\tag{20}
$$

$$
\begin{aligned}
C =& \frac{1}{2\ln 2}e^{\frac{1}{\alpha_1}}E_1(\frac{1}{\alpha_1}) + \frac{1}{2\ln 2}M\sum_{n=0}^{M-1}\binom{M-1}{n}\frac{(-1)^n}{n+1}e^{\frac{n+1}{\alpha_2}}E_1(\frac{n+1}{\alpha_2}) + [1-u_{nm}(n-m)]\binom{M-1}{n}\frac{(-1)^n M}{\alpha_2}\left[\alpha_1+(\alpha_1-1)e^{\frac{1}{\alpha_1}}E_1(\frac{1}{\alpha_1})\right]) \\
&- \frac{1}{2\ln 2}\Bigg(\sum_{n=0}^{M-1}\frac{u_{nm}}{\alpha_1}\binom{M-1}{n}(-1)^n M\left[\alpha_1 e^{\frac{1}{\alpha_1}}E_1(\frac{1}{\alpha_1}) - \frac{\alpha_2}{n+1}e^{\frac{n+1}{\alpha_2}}E_1(\frac{n+1}{\alpha_2})\right]\Bigg) \\
=& e^{\frac{1}{\alpha_1}}E_1(\frac{1}{\alpha_1})\{Q_1\} + \sum_{n=0}^{M-1} e^{\frac{n+1}{\alpha_2}}E_1(\frac{n+1}{\alpha_2})\{Q_2\} + \{Q_3\},
\end{aligned}
$$

where

$$
\begin{cases}
Q_1 &= \frac{1}{2\ln 2} - \sum_{n=0}^{M-1} f_n\left[u_{nm} + \frac{1-u_{nm}(n-m)}{\alpha_2}(\alpha_1-1)\right], \\
Q_2 &= f_n\left[\frac{1}{n+1} + \frac{u_{nm}}{\alpha_1}\frac{\alpha_2}{n+1}\right], \\
Q_3 &= -\sum_{n=0}^{M-1}\left[1-u_{nm}(n-m)\right] f_n\frac{\alpha_1}{\alpha_2}, \\
f_n &= \binom{M-1}{n}\frac{(-1)^n M}{2\ln 2}
\end{cases}
\tag{21}
$$

$$
u_{nm} = \begin{cases} \frac{1}{n-m} & \text{if } n \neq m \\ 0 & \text{if } n = m \end{cases} \tag{25}
$$

Then, $f_{\omega_{SR_\eta}+\omega_{R_\eta D}}$ is obtained by eq. (19). Based on eq. (19), we further derive $E_{\omega_{SR_\eta}+\omega_{R_\eta D}}\left\{\ln(1+\omega_{SR_\eta}+\omega_{R_\eta D})\right\}$, which is expressed in eq. (20). According to eqs. (7), (11), and (20), we derive the ergodic capacity of eq. (4), which is presented in eq. (21).

4. Simulations Results and Discussions

In the context of relaying networks with partial relay selection, we need to set some parameters for achieving the desired network performance. Key parameters, including the number of relays, transmit power levels, noise characteristics, and relay selection criteria should be carefully configured to strike a balance between data rate, outage probability, and symbol error rate while ensuring efficient and reliable data transmission. These settings play a pivotal role in tailoring the network to meet the specific requirements of the application and address challenges like channel impairments and interference. A well-optimized parameter configuration is essential to harness the full potential of relaying networks and provide robust and high-performing communication solutions for IoT and beyond.

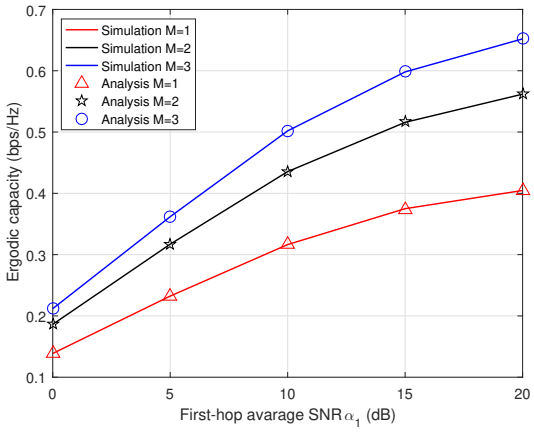

Figure 2. Effect of the average SNR α_1 on the ergodic capacity of the system, where $\alpha_2 = 0$ dB.

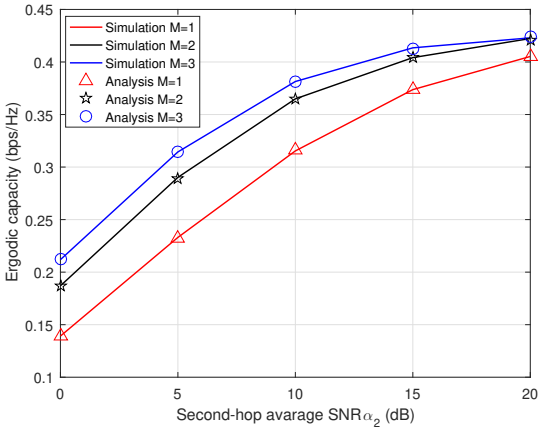

Figure 3. Effect of the average SNR α_1 on the ergodic capacity of the system, where $\alpha_2 = 0$ dB.

Table 1 Numerical effect of the average SNR α_1 on the ergodic capacity of the system, where $\alpha_2 = 0$ dB.

α_1 (dB)	0	5	10	15	20
Sim M=1	0.1387	0.2324	0.3164	0.3750	0.40
Ana M=1	0.1390	0.2323	0.3165	0.3735	0.40
Sim M=2	0.1863	0.3170	0.4355	0.5158	0.56
Ana M=2	0.1869	0.3162	0.4351	0.5170	0.56
Sim M=3	0.2118	0.3619	0.5019	0.5981	0.65
Ana M=3	0.2122	0.3618	0.5013	0.5984	0.65

Table 2 Numerical effect of the average SNR α_1 on the ergodic capacity of the system, where $\alpha_2 = 0$ dB.

α_2 (dB)	0	5	10	15	20
Sim M=1	0.1392	0.2331	0.3154	0.3737	0.40
Ana M=1	0.1390	0.2323	0.3165	0.3735	0.40
Sim M=2	0.1870	0.2902	0.3649	0.4041	0.42
Ana M=2	0.1869	0.2894	0.3646	0.4043	0.42
Sim M=3	0.2119	0.3144	0.3814	0.4135	0.42
Ana M=3	0.2122	0.3141	0.3808	0.4122	0.42

Fig. 2 and Table 1 present the effect of the average SNR α_1 on the ergodic capacity of the system, where $\alpha_2 = 0$ dB. From Fig. 2 and Table 1, we can find that the system capacity increases when α_1 increases. This is because that the increasing value of α_1 can effectively improve the transmission performance of the first hop, thus increasing the system capacity. Moreover, the system capacity also increases as the value of M increases. This is due to the relay selection, where a larger M means more available relays to be chosen, thereby improving the SNR of the second hop and further increasing the capacity of the whole system. In further, the simulated results match the analytical results very well, which verifies the effectiveness of the derived closed-form expressions of the ergodic capacity of the considered network.

Fig. 3 and Table 2 show how α_2 affects the ergodic capacity of the system, while holding α_1 at a constant value of 0 dB. As depicted in this figure and table, it is evident that the system capacity exhibits a notable upsurge as α_2 increases. This observed phenomenon can be attributed to the enhancement of the transmission capacity in the second hop of the communication process, contributing to an overall boost in the system capacity. Moreover, the system capacity demonstrates growth in proportion to an increase in the number of relays (M) due to the relay selection employed. Additionally, the remarkable agreement between the simulated and analytical results serves as strong validation for the accuracy of the derived expressions governing the system ergodic capacity, further reinforcing the reliability of our analysis and the practical applicability of the findings. This insight underscores the critical role of SNR, relay selection, and the number of relays in shaping the network capacity, which has significant implications for optimizing the performance of cooperative communication systems.

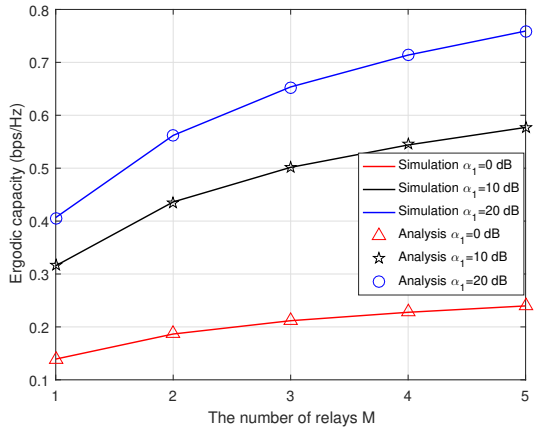

Figure 4. Impact of the number of relays M on the system ergodic capacity under different values of α_1, where $\alpha_2 = 0$ dB.

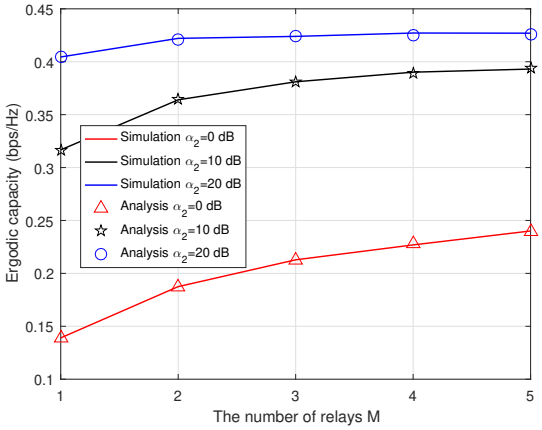

Figure 5. Impact of the number of relays M versus the system ergodic capacity under different values of α_2, where $\alpha_1 = 0$ dB.

Fig. 4 and Table 3 present the impact of the number of relays M on the system ergodic capacity under different average SNR α_1, where $\alpha_2 = 0$ dB. As described in Fig. 4 and Table 3, we can find that the ergodic capacity increases with the increasing value of M regardless of the value of α_1. This is due to the fact that increasing the number of relays M means that more available relays can be chosen in the dual-hop network, which greatly improves the transmission performance and therefore increases the system ergodic capacity. Moreover, the system performance performs better with a higher average SNR α_1, as a higher α_1 can help improve the capacity of the first-hop. Specifically, when $M = 5$, the ergodic capacity of $\alpha_1 = 20$ dB is highest, about 28% and 71% higher than those of $\alpha_1 = 10$ dB and $\alpha_1 = 0$ dB. Additionally, the simulated curves match the analytic curves very well, which verifies the effectiveness of the derived closed-form expression of the system ergodic capacity.

Table 3 Numerical impact of the number of relays M on the system ergodic capacity under different values of α_1, where $\alpha_2 = 0$ dB.

M	1	2	3	4	5
Sim α_1=0 dB	0.1392	0.1866	0.2117	0.2276	0.23
Ana α_1=0 dB	0.1390	0.1869	0.2122	0.2282	0.23
Sim α_1=10 dB	0.3155	0.4362	0.5015	0.5439	0.57
Ana α_1=10 dB	0.3165	0.4351	0.5013	0.5452	0.57
Sim α_1=20 dB	0.4067	0.5620	0.6535	0.7138	0.75
Ana α_1=20 dB	0.4048	0.5624	0.6527	0.7137	0.75

Table 4 Numerical impact of the number of relays M versus the system ergodic capacity under different values of α_2, where $\alpha_1 = 0$ dB.

M	1	2	3	4	5
Sim α_2=0 dB	0.1390	0.1875	0.2128	0.2269	0.24
Ana α_2=0 dB	0.1390	0.1869	0.2122	0.2282	0.23
Sim α_2=10 dB	0.3167	0.3640	0.3810	0.3901	0.39
Ana α_2=10 dB	0.3165	0.3646	0.3808	0.3888	0.39
Sim α_2=20 dB	0.4045	0.4221	0.4239	0.4271	0.42
Ana α_2=20 dB	0.4048	0.4210	0.4241	0.4254	0.42

Fig. 5 and Table 4 shows the impact of the number of relays M on the system ergodic capacity under different values of α_2, where $\alpha_1 = 0$ dB. It is evident from Fig. 5 and Table 4 that the system ergodic capacity increases with the increasing value of M irrespective of the specific α_2 setting. This is because that increasing the number of relays M means that more available relays can be chosen in the dual-hop network, which leads to substantial improvements in transmission

performance and therefore increases the system ergodic capacity. Moreover, it is worth noting that a higher α_2 results in a better system performance in ergodic capacity. Specifically, when $M = 4$, the ergodic capacity of $\alpha_2 = 20$ dB yields the highest ergodic capacity, about 12.5% and 46.2% higher than those of $\alpha_2 = 10$ dB and $\alpha_2 = 0$ dB. Additionally, the simulated curves closely align with the analytic curves, thereby validating the effectiveness of the derived closed-form expressions for the system ergodic capacity.

5. conclusion

This paper studied the integration of IoT transmission technology with multiple relays, for the enhancement of status monitoring for electrical equipment. Through an analytical analysis on the system data rate, we have demonstrated the advantages of employing partial relay selection in IoT-based electrical equipment monitoring. The results highlight the trade-offs between the system efficiency and performance, shedding light on the benefits of this approach for optimizing data transmission. By quantifying the improvements achieved through partial relay selection and assessing the impact of varying numbers of relays, our research can help reinforce the reliability of status monitoring in electrical systems. This work can serve as a significant step forward in advancing the capabilities of IoT solutions in the field of electrical equipment maintenance, providing a foundation for more efficient and effective monitoring systems in the future.

Acknowledgment

This work was supported by State Grid Sichuan Electric Power Company Science and Technology Project support (521901170004), where the project name is Hydropower Station operation and maintenance assistant decision system project based on real-time data.

5.1. Copyright

References

[1] Z. Huang, L. Bai, X. Cheng, X. Yin, P. E. Mogensen, and X. Cai, "A non-stationary 6g V2V channel model with continuously arbitrary trajectory," *IEEE Trans. Veh. Technol.*, vol. 72, no. 1, pp. 4–19, 2023.

[2] A. E. Haddad and L. Najafizadeh, "The discriminative discrete basis problem: Definitions, algorithms, benchmarking, and application to brain's functional dynamics," *IEEE Trans. Signal Process.*, vol. 71, pp. 1–16, 2023.

[3] R. Gabrys, S. Pattabiraman, and O. Milenkovic, "Reconstruction of sets of strings from prefix/suffix compositions," *IEEE Trans. Commun.*, vol. 71, no. 1, pp. 3–12, 2023.

[4] L. Liu, J. Zhang, S. Song, and K. B. Letaief, "Hierarchical federated learning with quantization: Convergence analysis and system design," *IEEE Trans. Wirel. Commun.*, vol. 22, no. 1, pp. 2–18, 2023.

[5] Y. Zheng, C. Wang, R. Yang, L. Yu, F. Lai, J. Huang, R. Feng, C. Wang, C. Li, and Z. Zhong, "Ultra-massive MIMO channel measurements at 5.3 ghz and a general 6g channel model," *IEEE Trans. Veh. Technol.*, vol. 72, no. 1, pp. 20–34, 2023.

[6] F. L. Andrade, M. A. T. Figueiredo, and J. Xavier, "Distributed banach-picard iteration: Application to distributed parameter estimation and PCA," *IEEE Trans. Signal Process.*, vol. 71, pp. 17–30, 2023.

[7] Q. Wang, S. Cai, Y. Wang, and X. Ma, "Free-ride feedback and superposition retransmission over LDPC coded links," *IEEE Trans. Commun.*, vol. 71, no. 1, pp. 13–25, 2023.

[8] Z. Xie, W. Chen, and H. V. Poor, "A unified framework for pushing in two-tier heterogeneous networks with mmwave hotspots," *IEEE Trans. Wirel. Commun.*, vol. 22, no. 1, pp. 19–31, 2023.

[9] T. Häckel, P. Meyer, F. Korf, and T. C. Schmidt, "Secure time-sensitive software-defined networking in vehicles," *IEEE Trans. Veh. Technol.*, vol. 72, no. 1, pp. 35–51, 2023.

[10] Y. Song, Z. Gong, Y. Chen, and C. Li, "Tensor-based sparse bayesian learning with intra-dimension correlation," *IEEE Trans. Signal Process.*, vol. 71, pp. 31–46, 2023.

[11] H. Wan and A. Nosratinia, "Short-block length polar-coded modulation for the relay channel," *IEEE Trans. Commun.*, vol. 71, no. 1, pp. 26–39, 2023.

[12] G. Zhang, C. Shen, Q. Shi, B. Ai, and Z. Zhong, "Aoi minimization for WSN data collection with periodic updating scheme," *IEEE Trans. Wirel. Commun.*, vol. 22, no. 1, pp. 32–46, 2023.

[13] A. Verma and R. Shrestha, "Low computational-complexity soms-algorithm and high-throughput decoder architecture for QC-LDPC codes," *IEEE Trans. Veh. Technol.*, vol. 72, no. 1, pp. 66–80, 2023.

[14] K. N. Ramamohan, S. P. Chepuri, D. F. Comesaña, and G. Leus, "Self-calibration of acoustic scalar and vector sensor arrays," *IEEE Trans. Signal Process.*, vol. 71, pp. 61–75, 2023.

[15] Q. Lu, S. Li, B. Bai, and J. Yuan, "Spatially-coupled faster-than-nyquist signaling: A joint solution to detection and code design," *IEEE Trans. Commun.*, vol. 71, no. 1, pp. 52–66, 2023.

[16] B. Han, V. Sciancalepore, Y. Xu, D. Feng, and H. D. Schotten, "Impatient queuing for intelligent task offloading in multiaccess edge computing," *IEEE Trans. Wirel. Commun.*, vol. 22, no. 1, pp. 59–72, 2023.

[17] X. Zhou, D. He, M. K. Khan, W. Wu, and K. R. Choo, "An efficient blockchain-based conditional privacy-preserving authentication protocol for vanets," *IEEE Trans. Veh. Technol.*, vol. 72, no. 1, pp. 81–92, 2023.

[18] D. Malak and M. Médard, "A distributed computationally aware quantizer design via hyper binning," *IEEE Trans. Signal Process.*, vol. 71, pp. 76–91, 2023.

[19] Y. Xiong, S. Sun, L. Liu, Z. Zhang, and N. Wei, "Performance analysis and bit allocation of cell-free massive MIMO network with variable-resolution adcs,"

IEEE Trans. Commun., vol. 71, no. 1, pp. 67–82, 2023.
[20] J. Shao, Y. Mao, and J. Zhang, "Task-oriented communication for multidevice cooperative edge inference," *IEEE Trans. Wirel. Commun.*, vol. 22, no. 1, pp. 73–87, 2023.
[21] H. H. López and G. L. Matthews, "Multivariate goppa codes," *IEEE Trans. Inf. Theory*, vol. 69, no. 1, pp. 126–137, 2023.
[22] H. Yao, X. Li, and X. Yang, "Physics-aware learning-based vehicle trajectory prediction of congested traffic in a connected vehicle environment," *IEEE Trans. Veh. Technol.*, vol. 72, no. 1, pp. 102–112, 2023.
[23] Q. Li, R. Gan, J. Liang, and S. J. Godsill, "An adaptive and scalable multi-object tracker based on the non-homogeneous poisson process," *IEEE Trans. Signal Process.*, vol. 71, pp. 105–120, 2023.
[24] F. Hu, Y. Deng, and A. H. Aghvami, "Scalable multi-agent reinforcement learning for dynamic coordinated multipoint clustering," *IEEE Trans. Commun.*, vol. 71, no. 1, pp. 101–114, 2023.
[25] H. Hui and W. Chen, "Joint scheduling of proactive pushing and on-demand transmission over shared spectrum for profit maximization," *IEEE Trans. Wirel. Commun.*, vol. 22, no. 1, pp. 107–121, 2023.
[26] W. Yu, Y. Xi, X. Wei, and G. Ge, "Balanced set codes with small intersections," *IEEE Trans. Inf. Theory*, vol. 69, no. 1, pp. 147–156, 2023.